Evolution, 2023, **XX(XX)**, 1–13
https://doi.org/10.1093/evolut/qpac052
Advance access publication 22 December 2022
Original Article

OXFORD

Morphological integration during postnatal ontogeny: implications for evolutionary biology

Alex Hubbe, PhD[1,2], Fabio A. Machado, PhD[3], Diogo Melo, PhD[4], Guilherme Garcia, PhD[5], Harley Sebastião, PhD[5], Arthur Porto, PhD[6,7], James Cheverud, PhD[8], Gabriel Marroig, PhD[5]

[1]Staatliches Museum für Naturkunde Stuttgart, Stuttgart, Germany
[2]Departamento de Oceanografia, Instituto de Geociências, Universidade Federal da Bahia, Bahia, Brazil
[3]Department of Integrative Biology, Oklahoma State University, Stillwater, Oklahoma, United States
[4]Lewis-Sigler Institute for Integrative Genomics, Princeton University, Princeton, New Jersey, United States
[5]Departamento de Genética e Biologia Evolutiva, Instituto de Biociências, Universidade de São Paulo, São Paulo, Brazil
[6]Department of Biological Sciences, Louisiana State University, Baton Rouge, Louisiana, United States
[7]Center for Computation and Technology, Louisiana State University, Baton Rouge, Louisiana, United States
[8]Department of Biology, Loyola University Chicago, Chicago, Illinois, United States

Corresponding author: Staatliches Museum für Naturkunde Stuttgart, Rosenstein 1, 70191 Stuttgart, Germany; Departamento de Oceanografia, Instituto de Geociências, Universidade Federal da Bahia, Bahia 40170-020, Brazil. Email: alexhubbe@yahoo.com

Abstract

How covariance patterns of phenotypes change during development is fundamental for a broader understanding of evolution. There is compelling evidence that mammalian cranium covariance patterns change during ontogeny. However, it is unclear to what extent variation in covariance patterns during ontogeny can impact the response to selection. To tackle this question, we explored: (a) the extent to which covariance patterns change during postnatal ontogeny; (b) in which ontogenetic stages covariance patterns differ the most; and (c) the extent to which the phenotypic covariance pattern at different ontogenetic stages can be explained by the same processes determining additive genetic covariance. We sampled the postnatal ontogenetic series for both marsupials and placentals. Within each ontogenetic series, we compared covariance matrices (**P**-matrices) at different ontogenetic stages. Furthermore, we compared these **P**-matrices to two target matrices [adult **P**-matrix and an additive genetic covariance matrix (**G**-matrix)]. Our results show that for all ontogenetic series, covariance patterns from weaning onward are conserved and probably shaped by the same processes determining the **G**-matrix. We conclude that irrespective of eventual differences in how selection operates during most of the postnatal ontogeny, the net response to such pressures will probably not be affected by ontogenetic differences in the covariance pattern.

Keywords: development, **G**-matrix, **P**-matrix, Marsupialia, Placentalia

Developmental processes change the amount and distribution of morphological variation through time (Mitteroecker & Bookstein, 2009; Zelditch et al., 2006). Not surprisingly, this is well documented for the mammalian cranium (Atchley, 1984; Coleman et al., 1994; Goswami et al., 2012; Hallgrímsson et al., 2009; Mitteroecker & Bookstein, 2009; Mitteroecker et al., 2012; Nonaka & Nakata, 1984; Sydney et al., 2012; Zelditch, 1988; Zelditch & Carmichael, 1989; Zelditch et al., 1992, 2006), which is a common model system for investigating the evolution of complex structures [e.g., Goswami (2006); Haber (2015); Machado et al., (2018)]. Yet, there is little evidence on how these documented differences along ontogeny would affect evolution.

Since natural selection is contingent on the availability and organization of morphological variation (Lande, 1979; Lande & Arnold, 1983), differences in the amount and structure of variation across life history stages can affect how populations respond to selection (Wasserman et al., 2021). For example, consider a scenario in which a pair of traits are associated (i.e., high integration *sensu* Olson & Miller, 1958) in the juvenile phase, but in the adult phase, these traits are much less integrated [Figure 1; e.g., Sydney et al. (2012)]. If selection operates on a single trait at the juvenile stage, evolutionary responses will be aligned with the major direction of variation of juveniles, leading to a correlated response in the second trait, even in the absence of trait association in the adult phase. Furthermore, in this scenario, the reconstruction of selection using the adult stage would suggest that selection is acting on multiple traits simultaneously, while in fact, it is acting on a single trait earlier in development. Conversely, if the covariance patterns are relatively stable throughout ontogeny, selection would produce evolutionary responses that are similar across ontogenetic stages. Therefore, understanding how the variance is distributed on different ontogenetic stages can provide further insight about how complex phenotypes might evolve in response to natural selection. This knowledge has also broader implications since complex phenotypes play, for instance, an important role in ecological interactions (Assis et al., 2022; Saccheri & Hanski, 2006), and population's extinction risk (Forester et al., 2022).

Received May 2, 2022; accepted December 2, 2022

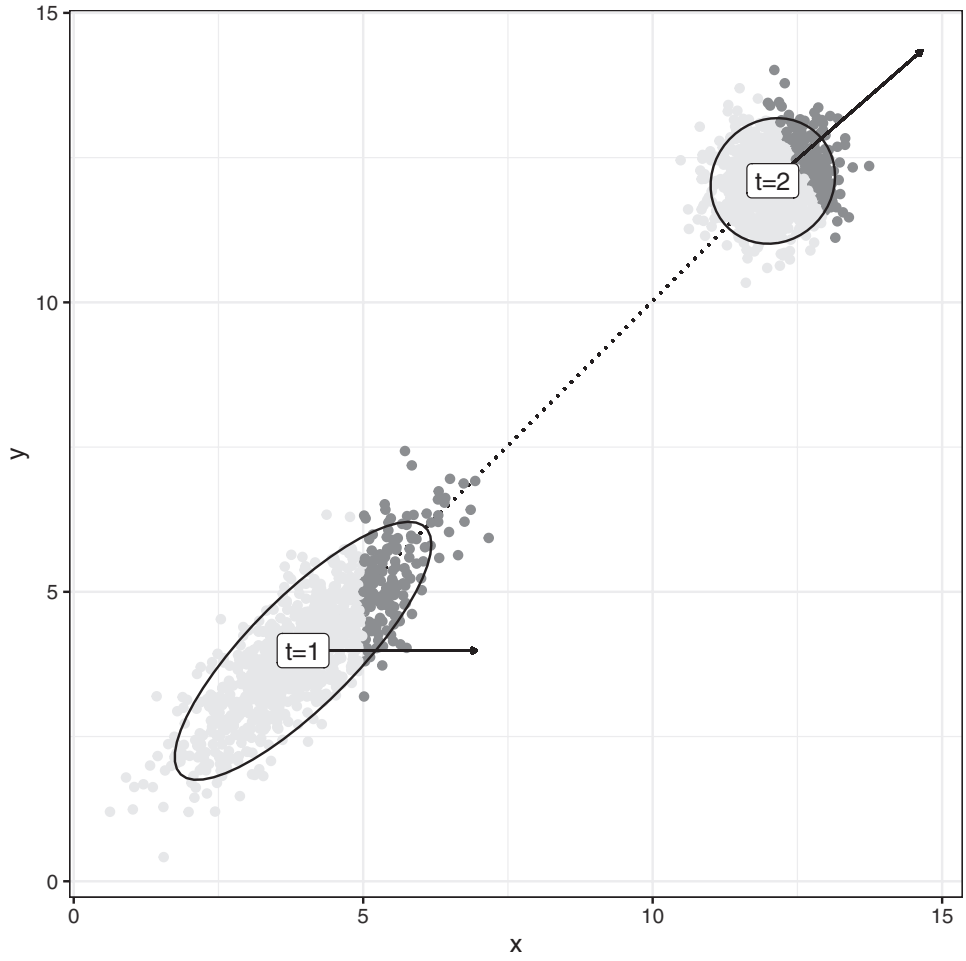

Figure 1. Effect of ontogenetic changes in covariance patterns on the evolutionary response of life history stage specific selection. Population is sampled in two moments: $t = 1$ with strong integration and $t = 2$ with weak integration. At $t = 1$, the selection gradient (solid arrow) affects only the trait x (dark gray specimens), resulting in a selection differential that is correlated between x and y due to the high integration. At $t = 2$, because x and y are not correlated, the reconstructed selection gradient (solid arrow) indicates that both traits were co-selected (dark gray specimens), while in fact, only x was.

Here, we explore whether the observed variation in covariance patterns during postnatal ontogeny can influence evolution in age-structured populations under directional selection by assessing: (a) the extent to which covariance patterns change during postnatal ontogeny; (b) in which ontogenetic stages covariance patterns differ the most (if they do at all), and (c) the extent to which the phenotypic covariance pattern at different ontogenetic stages mirrors the additive genetic covariance matrix (**G**-matrix). This last point serves a dual purpose. First, it tests if the structuring of phenotypic variation in different life history stages is given by the underlying gene-phenotypic map of those traits, and if there is a possibility that the gene-phenotypic map is changing throughout ontogeny, for example, through differential gene expression. Second, if **G**-matrices are similar to age-specific **P**-matrices, then it is possible that age-specific **G**-matrices are stable throughout ontogeny, implying that the same selective pressure applied on different stages will lead to similar adaptive responses.

To explore these questions, we developed a cross-sectional study of cranial trait covariances based on a sample of mammals with different developmental strategies. We sampled the Didelphimorphia marsupials *Didelphis virginiana* and *Monodelphis domestica*, the precocial platyrrhine primate *Sapajus apella*, and the altricial sigmodontinae rodent *Calomys expulsus* in different age classes encompassing the first months of life after birth to adulthood. We quantified covariance patterns of cranial morphological traits and used published estimates of additive genetic covariance matrices for the same species or relatively closely related taxa. Next, we compared covariance patterns among age classes within each one of these ontogenetic series to evaluate if observed differences across age classes would produce different evolutionary responses under selection.

Methods

Sample

Our sample is composed of 1,883 specimens belonging to five ontogenetic series: *D. virginiana* and *M. domestica* (Marsupialia, Mammalia), *S. apella* (Primates, Placentalia, Mammalia), and *C. expulsus* (Rodentia, Placentalia, Mammalia; Figure 2). Studied specimens are deposited in the following institutions: American Museum of Natural History (New York, USA), Field Museum of Natural History (Chicago, USA), Museu Nacional (Rio de Janeiro, Brazil), Museu Paraense Emilio Goeldi (Belém, Brazil), Museu de Zoologia da Universidade de São Paulo (São Paulo, Brazil), Museum of Vertebrate Zoology (Berkeley, USA), National

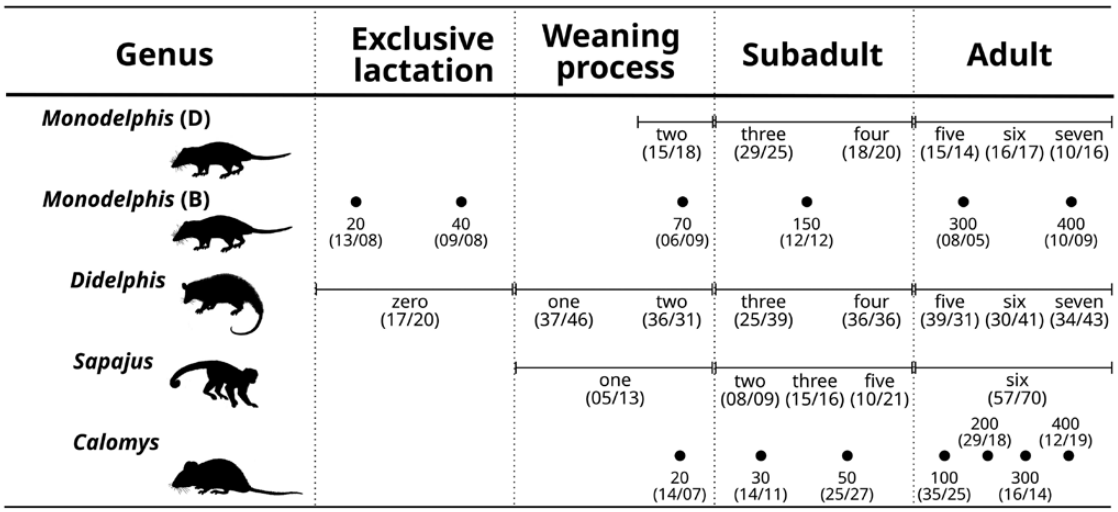

Figure 2. Schematic representation of the age classes and sample sizes (between parentheses) for each ontogenetic series in relation to major life history phases. Birth age classes are represented by dots and dental age classes by horizontal bars. The position of these symbols and the length of the bars are pictorial and intended to show the broad distribution of data over the major life history phases and the differences in both sampling strategies (dental and birth age classes). Figures for each ontogenetic series are adapted from (Eisenberg, 1989; Eisenberg & Redford, 1999; Redford & Eisenberg, 1992). Figures not to scale.

Museum of Natural History (Washington D.C., USA), and Texas Biomedical Research Institute (San Antonio, USA).

We worked with specimens that were: (a) wild caught (*Didelphis*, *Monodelphis*, and *Sapajus*), and represent more than one population per species; or (b) derived from captive-bred colonies kept under stable controlled conditions and founded based on a single population [*Calomys* (Garcia et al., 2014) and *Monodelphis* (Porto et al., 2015; VandeBerg & Robinson, 1997)]. The two independent data sets for *Monodelphis* were labeled *Monodelphis* (D) for the wild-caught specimens and *Monodelphis* (B) for the captive-bred specimens. The acronyms stand for dental age class and birth age class, respectively, as explained below.

We classified our specimens according to age classes. Wild-caught specimens were classified according to dental eruption and wear (i.e., dental age class), while captive-bred specimens were classified according to days after birth (i.e., birth age class; Figure 2). Dental age classes for *Didelphis* and *Monodelphis* (D) were determined based on maxillary dental eruption and wear (Tribe, 1990; Tyndale-biscoe & Mackenzie, 1976). We added an extra class (zero), composed of specimens with no erupted teeth. For *Didelphis*, the ontogenetic stages sampled most likely include lactation (dental age class zero), the start of solid food ingestion (dental age class one), end of the weaning (between dental age classes one and two), to adulthood [dental age class above four; Abdala et al. (2001); McManus (1974); Sebastião & Marroig (2013); Tyndale-biscoe & Mackenzie (1976); van Nievelt & Smith (2005)].

For *Monodelphis* (D), the ontogenetic stages sampled most likely include the end of the weaning process (during dental age class two) to adulthood [dental age class above four; Sebastião & Marroig (2013); van Nievelt & Smith (2005)]. *Monodelphis* (B) specimens were classified according to birth age classes 20, 40, 70, 150, 300, and 400 days after birth. These classes encompass exclusive lactation (20 and 40), to the very end of the weaning process (70), and to adulthood [300 and 400; Nievelt & Smith (2005)]. The birth age classes are analog to the following dental age classes: 20 = zero; 40 = zero to one; 70 = two; and ≥ 150 ≥ four (Nievelt & Smith, 2005; van Nievelt & Smith, 2005). The dental age classes for *Sapajus* were determined based on the premaxillary and maxillary dental eruption (Richtsmeier et al., 1993). They span from weaning (dental age class one) to adulthood [dental age class six; Fragazy et al. (2004); Marroig & Cheverud (2001)]. The *Calomys* were classified according to the birth age classes 20, 30, 50, 100, 200, 300, and 400 days after birth. Specimens comprise from around weaning (20 days) to adulthood [100 days onwards; Hingst-Zaher et al. (2000)].

For *Sapajus*, almost all specimens we studied are assigned to *S. apella* (n = 200), however, 24 specimens are of uncertain classification (*Sapajus* sp.). These specimens belong to the age classes one (n = 6), two (n = 11), and three (n = 7). Inspections of principal component analysis (PCA) plots showed that specimens with unknown species fell within the distribution of *S. apella*, cluster along other juveniles (Supplementary Figure A1). A nonparametric multivariate analysis of variance (NP-MANOVA, Anderson, 2001; Collyer & Adams, 2018; McArdle & Anderson, 2001) using size (to control for ontogenetic variation) and species assignment as factors showed no differentiation between *S. apella* and *Sapajus* sp. (Supplementary Table A1). Based on these results, we pooled both groups in our analysis to increase sample sizes.

The ontogenetic series from *Didelphis*, *Monodelphis* (B), *Calomys*, and *Sapajus* and adults from *Monodelphis* (D) were already used in previous studies for other purposes (Garcia et al., 2014; Marroig, 2007; Marroig & Cheverud, 2001; Porto et al., 2015; Sebastião & Marroig, 2013), while data from *Monodelphis* (D) (excluding adults) are presented here for the first time.

Landmarks and measurements

The traits in this study are linear distances derived from the 3D coordinates of 32 homologous landmarks measured on all specimens using a 3D digitizer. All specimens were measured with the same instrument (Microscribe MX; Immersion Corporation, San Jose, California) with the exception of adult *Sapajus* that were measured with a 3Draw digitizer (Polhemus Inc., Colchester, Vermont). Based on these landmarks, 35 linear distances were calculated in

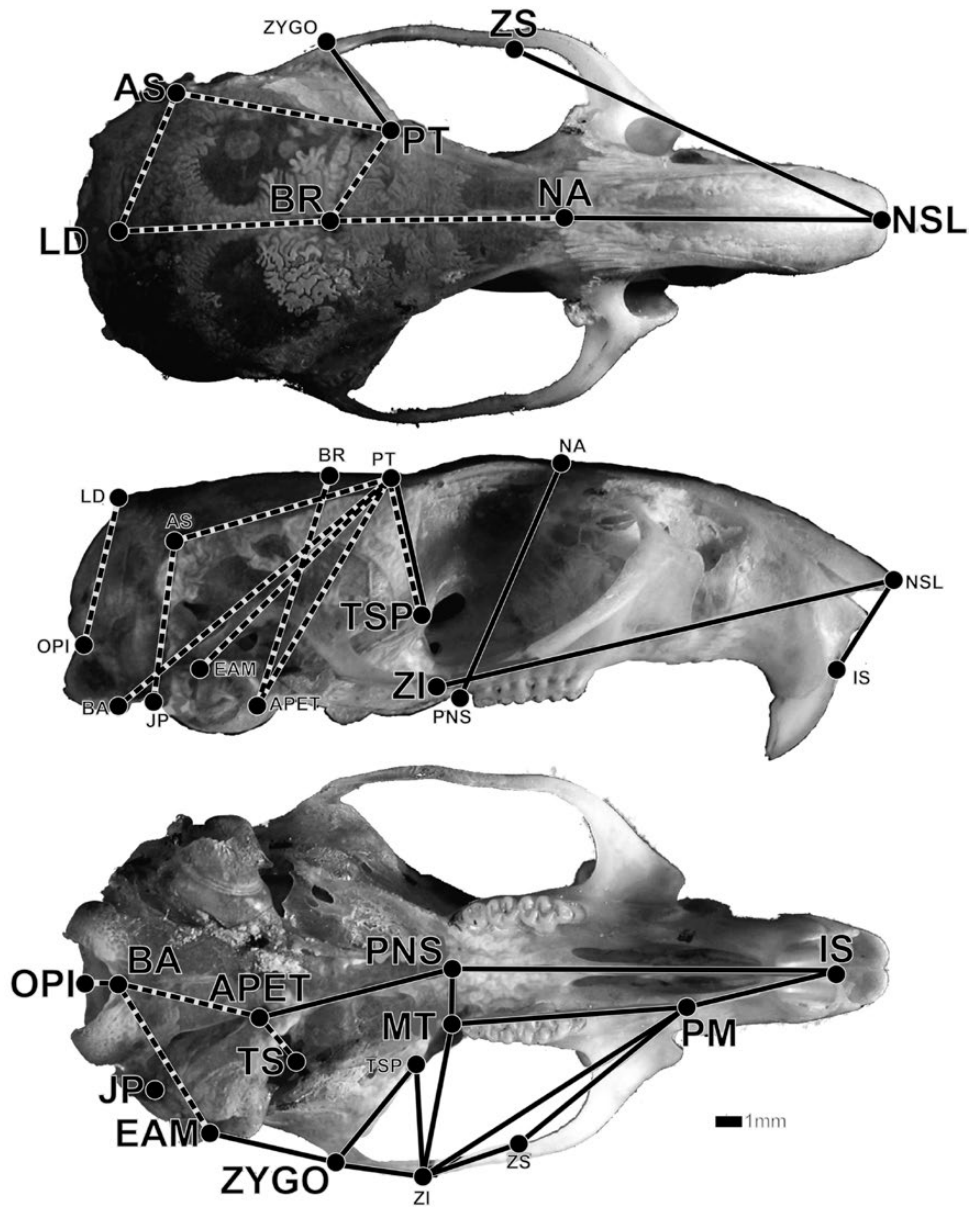

Figure 3. Location of the landmarks registered and the set of 35 interlandmark linear distances derived from these landmarks over an adult skull of *Calomys expulsus* in dorsal (A), lateral (B), and ventral (C) views. Landmark names are highlighted in the particular view at which they are best defined. Solid line: linear distance associated with the facies; doted line: linear distance associated with the neurocranium. Figure adapted from (Garcia et al., 2014).

millimeters [Figure 3; for details related to the landmarks and distances acquisition refer to Cheverud (1995); Porto et al. (2009); Shirai & Marroig (2010)]. The set of distances calculated aimed to represent the whole cranium morphology and important developmental and functional relationships among cranial regions, while avoiding redundancy and focusing on individual bones or localized developmental processes (Cheverud, 1982; Marroig & Cheverud, 2001).

Some sources of measurement error could introduce non-biological variance in our data sets. First, more than one piece of equipment was used to collect data. However, tests performed with adult specimens measured with both devices indicated that this source of variation is negligible. Second, specimens were measured by different observers. *Didelphis* and *Monodelphis* (D) crania were measured by HS. *Monodelphis* (B) crania were measured by AP. *Calomys* crania were measured by GG, and *Sapajus* crania were measured by GM. Nevertheless, all specimens were measured following the same protocol, and since we are studying covariances within each ontogenetic series, and all specimens per ontogenetic series were measured by the same person, we expect an interobserver error to be irrelevant.

Lastly, to evaluate the possible effect of within-sample measurement error in covariance estimates we calculated trait repeatabilities (Lessells & Boag, 1987) for samples that were measured twice, namely, *Didelphis*, *Monodelphis* (D), and *Calomys*. Measurement errors were calculated for each ontogenetic series at each age class with more than 14 specimens for each linear distance independently. In most cases, measurement errors are negligible, since most repeatabilities were high (> 0.8 Supplementary Figure A2). Low

repeatabilities (< 0.8) were observed for traits exhibiting low variances (Supplementary Figure A3). These traits were also very short, approaching the spatial resolution of the digitizer (Supplementary Figure A3). In all subsequent analyses, specimens' traits were represented by the mean of replicated measurements. Although the *Sapajus* and the *Monodelphis* (B) specimens were not measured twice, the measurement errors observed for other Platyrrhini measured by GM (Marroig & Cheverud, 2001), and for smaller Didelphimorphia measured by AP (Porto et al., 2009) were negligible. Therefore, we assume the *Sapajus* and *Monodelphis* (B) specimens also presented negligible measurement errors.

Furthermore, all downstream analyses were repeated for a smaller set of traits (15 and 5 traits; Supplementary Table A2). We chose distances that had the highest measurement repeatability on all species, and that had a fairly equal coverage over different parts of the cranium. Their results are in agreement with our interpretation for the 35 traits (see "Results" for details).

Phenotypic covariance matrices

Our study is concerned with how the association among traits changes during ontogeny. To quantify trait associations, we calculated phenotypic covariance matrices (**P**-matrices) of each age class per ontogenetic series. Because our sample includes both male and female specimens (Supplementary Table A3), we evaluated if the presence of sexual dimorphism could affect our covariance estimation.

To verify this possibility, we used the following approaches. First, we used pairwise NP-MANOVA (significance at $p(\alpha) < 0.05$) to evaluate the effect of sex on morphology for each age class. In cases of insufficient sample sizes for NP-MANOVA we used pairwise non-parametric univariate analysis of variance (NP-ANOVA), and considered sexual dimorphism to be present whenever two or more traits had significantly covaried with sex at $p(\alpha) < 0.01$. Second, sexual dimorphism was also graphically evaluated using PCA. Lastly, we assessed the impact that controlling for sexual dimorphism has on the covariance estimates by evaluating the extent to which the covariance structure is altered by the exclusion of sex in the analyses. To do that, first we calculated matrices with and without controlling for sexual dimorphism and compared them using the random skewers (RS) method (for details on the method see below) and also calculating the difference between the trace of the matrices. Because sexual dimorphism was identified as a source of variance in at least one age class per ontogenetic series, we calculated the residual pooled within-group **P**-matrices for all samples using the linear model approach. The linear model for each ontogenetic series and age class considered sex as the predictor variable and the matrix of the 35 linear distances for each individual as the response variable. For the adult age class, which combines more than one age class (Figure 2), we considered sex, age class, and their interaction as predictors. This step is important because if an effect is a strong source of variance, it distorts matrix estimates, which will reflect inter-group (e.g., female and male differences) instead of intra-group covariances [see Figure SI1 in Machado et al. (2018)].

For the same reason, we explored whether between-population differences could bias the matrix estimates by stratifying wild-caught specimens by geographic location. For all species, there was considerable morphological overlap between specimens taken from multiple locations (Supplementary Figure A4). An NP-MANOVA controlling for size shows that, even though there is a significant effect of location, this factor explained a small portion of the total variation in the sample [< 6 %, (Supplementary Table A4)], rendering it unlikely that the patterns we observe are being shaped by between-population variation in wild species.

Any matrix is estimated with error, and the lower the ratio between the number of traits and sample size the worst is the estimation. We took uncertainty in matrix estimation into account by using a Bayesian posterior sample of the covariance matrices derived from a multivariate normal likelihood function on the residuals of the linear models and an inverse Wishart prior on the covariance structure. The prior covariance matrix is set to a diagonal matrix with the observed variances on the diagonal, and the prior degrees of freedom is set to the number of traits ($k = 35$). This particular choice for the likelihood and prior distribution can be solved analytically and results in a posterior distribution from which we can sample directly (Murphy, 2012). Furthermore, this method has the added benefit of ensuring that the matrices from the posterior sample are positive-definite and, therefore, invertible. We took 100 posterior samples for each age class from each ontogenetic series, producing 3,600 matrices in total.

To visualize differences and similarities between the **P**-matrices we performed a principal coordinate analysis (PCoA). The PCoA transforms the original dimensionality of a multivariate dataset in a manner that a lower-dimensional representation can be adopted, similarly to the PCA. Different from PCA, the PCoA is based on the spectral decomposition of the double-centered distance matrix that represents the dissimilarities among samples. The eigenvectors of this analysis (principal coordinates; PCo) express the scores of each sample on this reduced space, with the leading eigenvectors representing the axes in which covariance matrices differ the most, and the latter representing the axes in which they differ the least. The dissimilarity between matrices was calculated based on the Riemannian distance, which is the metric of the space of square symmetric positive definite matrices (Bookstein & Mitteroecker, 2014; Le Maître & Mitteroecker, 2019; Mitteroecker, 2009). Because Riemannian distances matrices are sensitive to scale, matrices were set to have the same size (trace = 1) prior to the calculation. The resulting PCo space then only relates to the matrix shape.

Additive genetic covariance matrices

The **P**-matrix is determined by the additive genetic covariance matrix (**G**-matrix), plus the environmental covariance (Falconer & MacKay, 1996). The **G**-matrix quantifies the genetic contribution to a trait's patterns of inheritance and co-inheritance (covariance) and is essential for predicting the multivariate evolution of these traits (Falconer & MacKay, 1996; Lande, 1979; McGuigan, 2006). Because of that, we evaluated if patterns of covariance quantified in our age-specific **P**-matrices can be explained by the distribution of heritable variation encoded in the **G**-matrix. To do this, we compared our age-specific **P**-matrices within the ontogenetic series with estimated target **G**-matrices (see details regarding the comparison method below). The reasoning behind this approach is that since **G**-matrices of complex traits represent the net effect of multiple pleiotropic effects channeled through developmental pathways (Cheverud, 1996a), finding a high similarity between the age-specific **P**-matrices and the target **G**-matrix means that trait associations within **P**-matrices are probably determined by the same processes determining the **G**-matrix pattern.

Obtaining **G**-matrices is a complex endeavor (Gervais et al., 2019; McGuigan, 2006; Steppan et al., 2002), and **G**-matrices for mammalian crania are rare. For that reason, depending on the ontogenetic series, a different target **G**-matrix was adopted. For comparisons within Didelphimorphia [*Didelphis*, *Monodelphis* (D), and *Monodelphis* (B)], we used a matrix for *M. domestica* (Porto et al., 2015); and for the comparison within *Calomys*, we used a matrix estimated for the same species (Garcia et al., 2014). These matrices were estimated using the same individuals from the *Monodelphis* (B) and *Calomys* ontogenetic series, respectively. There is no available **G**-matrix for *Sapajus*. Therefore, we used a matrix estimated for *Saguinus* (Cheverud, 1996b), which is the only available **G**-matrix for New World Monkeys (Marroig & Cheverud, 2010).

There is a considerable difference in size between *Saguinus*, and *Sapajus*, and *Monodelphis* and *Didelphis* (Jones et al., 2009), which results in larger variances and covariances for the larger species (*Sapajus* and *Didelphis*). Nevertheless, the methods employed to compare matrices (see below) are primarily concerned with the directions (and not magnitudes) of variances and covariances in the morphospace, and differences due to size do not influence our results.

The **G**-matrix for *Calomys* was estimated from 365 specimens comprising individuals of both sexes and of different age classes, and that were raised in an unbalanced colony design (i.e., containing both paternal and maternal half-sibs). The **G**-matrix for *Monodelphis* was estimated from 199 adult specimens belonging to 16 partially inbred strains. Both matrices were estimated using a Bayesian sparse factor model (Runcie & Mukherjee, 2013), in a full animal model for *C. expulsus* (Garcia et al., 2014) and a structured random effect model for *M. domestica* that used the genetic distance between strains to define the covariance between random effect levels (Porto et al., 2015). For *Saguinus*, the **G**-matrix was estimated from 462 specimens pooled from two different species: *S. oedipus* and *S. fuscicollis*. Pooling species for quantitative genetic estimates can be problematic, but given that covariance patterns seem to be stable through the new-world monkey radiation (Marroig & Cheverud, 2001), we don't expect this to have a large influence on the estimated matrix. Colony designs were unbalanced, including full- and half-siblings, and various kinds of collateral relatives. The matrix was estimated under a maximum likelihood framework in a full animal model (Cheverud, 1996b; Konigsberg & Cheverud, 1992). In all cases, unwanted sources of variation, like sex and species (in the case of *Saguinus*), were controlled using fixed effects.

Matrix comparisons

To evaluate how much covariance patterns change during ontogeny, we compared age-specific **P**-matrices within ontogenetic series using two different approaches: the Krzanowski subspace comparison for multiple matrices (KC; (Aguirre et al., 2014; Krzanowski, 1979) and the RS (Cheverud & Marroig, 2007).

We used KC to compare age-specific **P**-matrices within each of the five ontogenetic series (Figure 2). KC is a global test of similarity among all matrices, and it is intended to evaluate if there is any significant deviation from equality within our ontogenetic series phenotypic matrix samples. It measures the alignment of the morphospaces spanned by the first few eigenvectors of the matrices being compared. Structurally similar matrices should have most of their variation in a similar subspace. The matrix that describes the common subspace is defined as

$$H = \sum_{i=1}^{p} A_i A_i^t \tag{1}$$

where A_i is a column matrix containing the first $k = n/2 - 1$ eigenvectors of the ith matrix being compared, p is the number of matrices being compared, and t denotes matrix transposition. The eigenvalues of H are at most p, and any eigenvector of H whose associated eigenvalue is equal to p can be reconstructed by a linear combination of the eigenvalues included in the A_i matrices, and so is shared by all the matrices.

To create a null distribution for the eigenvalues of H, we used a permutation approach (Aguirre et al., 2014). We created 1,000 permutations of the pooled residuals from the fixed effect models used to calculate the **P**-matrices for the age classes within each ontogenetic series. For each permuted sample, we repeat the Bayesian posterior sampling of the **P**-matrix in each age class and calculate the H matrix. This provides a null distribution for the eigenvalues of H under the hypothesis that the residuals for each age class came from the same population. The confidence intervals in the observed H matrix are obtained using the posterior distribution of the true **P**-matrices, while the permuted confidence interval under the null hypothesis combines the uncertainty from the randomization and from the posterior distributions for each randomized sample. If the observed eigenvalues of H were significantly different from the randomized eigenvalues, we concluded that the matrices from each age class have a different structure, otherwise, we concluded that the matrices are similar.

Additionally, we used the RS method to compare the median of each posterior distribution of age-specific **P**-matrices within each ontogenetic series against two target matrices: the median of the posterior distribution of the adult pooled within-group **P**-matrix of each ontogenetic series and a **G**-matrix (see above for details on the **G**-matrices compared in each case). This was done for three main reasons. First, we intend to evaluate if age-specific matrices are similar to the adult **P**, the matrix which is usually the focus of studies on morphological integration. Second, we compared age-specific matrices to a target **G**-matrix to evaluate if the **P**-**G** similarity already described for adults (Hubbe et al., 2016; Marroig & Cheverud, 2010; Porto et al., 2015) holds for all sampled age classes. Lastly, the RS was chosen for this task, instead of KC, because it provides a more intuitive picture of the evolutionary consequences of matrix similarity and dissimilarity. RS is based on the following equation:

$$r_i = \mathbf{C}_i v \tag{2}$$

where v is a random vector, $\mathbf{C_i}$ is a matrix being compared, and r_i is the response vector. The RS similarity is then defined as the mean vector correlation between the response vectors obtained by applying the same set of random vectors to two covariance matrices (Cheverud & Marroig, 2007; Melo et al., 2015). If the covariance matrices have similar structures, their response vectors will be closely aligned and the RS will be close to 1. If they have unrelated structures, the direction of the response will be different and the RS will be close to zero.

For reasonably similar matrices, as in our case, r is strongly and negatively correlated to the Riemannian distance (Supplementary Figure A5), with the advantage that, under certain conditions, RS has a straightforward biological interpretation. The RS equation has the same format as the multivariate response to the selection equation $\Delta z = \mathbf{G}\beta$ (Lande, 1979), where β is the selection gradient (direction of maximum fitness increase), **G** is the **G**-matrix and Δz is the evolutionary response to the selection vector. Thus, for evolutionary studies, RS is a measure of the average alignment between the evolutionary responses of two populations subjected to the same selective pressures. We can calculate this if we have access to the **G**-matrices or to **P**-matrices that are good proxies for the corresponding **G**-matrices. This is why we compared the age-specific **P**-matrices within the ontogenetic series not only with adult **P**-matrices, which allows us to scrutinize phenotypic differences in covariance patterns within the ontogenetic series, but also with **G**-matrices.

As explained above, if the RS for age-specific **P**-matrices within ontogenetic series are similar to the target **G**-matrices, we can infer that the phenotypic covariance patterns within each ontogenetic series can be sufficiently explained by the same processes determining the (co)inheritance of traits. Furthermore, this similarity would also suggest that different age classes respond similarly to selection. The proportionality between **P**- and **G**-matrices, sometimes referred to as the *Cheverud Conjecture* (Roff, 1995), has been verified for adult cranial traits in many lineages of mammals (Cheverud, 1995; Hubbe et al., 2016; Machado et al., 2018; Marroig & Cheverud, 2001; Oliveira et al., 2009; Porto, 2009; Shirai & Marroig, 2010), and specifically for the lineages investigated here (Cheverud, 1995; Garcia et al., 2014; Marroig & Cheverud, 2010; Porto et al., 2015). Thus, by evaluating the RS similarity between age-specific **P**-matrices within ontogenetic series and target **G**-matrices, we are also testing if the Cheverud conjecture can be extended to other ontogenetic stages besides the adult one.

Due to sampling error associated with the estimation of covariance matrices, the maximum RS value (r_{max}) between two matrices will never be one, even if the underlying samples come from the same population. To account for this, we calculated matrices repeatabilities (t), which is a measure of the expected similarity between the true underlying covariance structure and the one calculated from the sample. The t value for all matrices was determined using a Monte-Carlo resampling procedure of self-correlation (Marroig & Cheverud, 2001; Porto et al., 2009). For every covariance matrix, 1,000 Monte Carlo samples were made keeping the sample size constant. Repeatabilities for the *Calomys* and *Monodelphis* **G**-matrices were calculated using the published effective sample sizes, and the one for *Saguinus* was taken from the literature (Cheverud, 1996b; Marroig & Cheverud, 2010). Covariance matrices were estimated for each of the resamples and RS was used to compare the original and the resampled matrices. The t value was then obtained as the mean RS value between the original and resampled matrices. Adjusted RS similarity was then estimated as $r_{adj} = r_{obs}/r_{max}$, where r_{obs} is the observed similarity among samples and r_{max} is the geometric mean of ts of the pair of matrices being compared (Cheverud, 1996b). The procedure described above provides inflated estimates of repeatabilities for poorly estimated **P**-matrices, thus providing conservative corrections for RS when at least one poorly estimated **P**-matrix is considered in the analysis.

Lastly, both KC and RS are primarily concerned with the directions of variance in the morphospace. Magnitudes of variance are strongly correlated with the scale of the organisms, which changes considerably across different age classes. More specifically, KC considers only the eigenvectors (directions) of the matrices under study, disregarding the corresponding eigenvalues (variance in these directions); and RS considers the direction and magnitude of covariance patterns, but quantifies only the alignment (directions) of response vectors, and not their length (magnitude). In other words, the RS similarity depends on the relative distribution of variances, not on its magnitude.

Statistical analyses

All analyses were done in the R Core Team (2019) programming environment. The EvolQG v0.3-1 (Melo et al., 2015) package was used for matrix estimation, RS and KC comparisons, the package RRPP (Collyer & Adams, 2018) was used for the NP-ANOVAs and NP-MANOVAs and the package vcvComp (Le Maître & Mitteroecker, 2019) was used for the PCoA. Analyses were done independently by three authors (F.A.M., D.M., and G.G.), and the results were consistent between runs.

Results

The first two leading eigenvectors of the PCoA explained 29.97% and 4.11% of the total variation in the sample, respectively (Figure 4). PCo1 separates *Didelphis* and *Sapajus* samples with higher scores from *Monodelphis* (B), *Monodelphis* (D), and *Calomys* samples with lower scores. PCo2 shows a contrast between *Monodelphis* (B), *Monodelphis* (D), and *Didelphis* with lower scores from *Calomys* and *Sapajus* with higher ones. PCo1 presents some ontogenetic structuring of the marsupial species, with younger age classes showing lower values than adult classes. Furthermore, the *Monodelphis* (B) and *Monodelphis* (D) form almost a continuum, with the latter stages of *Monodelphis* (B) neighboring intermediary to the late stages of *Monodelphis* (D). The following eigenvectors explained < 3 % of the total variation and show no clear taxonomic or ontogenetic structure (Supplementary Figure A6).

The KC analysis shows that the posterior eigenvalue distribution fully overlaps with the null distribution for all ontogenetic series (Figure 5), suggesting that, despite the dispersion observed in Figure 4 for some age classes, covariance structures tend to be similar within ontogenetic series. The only possible exception is within the *Monodelphis* (B), where the posterior distribution of the leading eigenvalue falls partly outside of the null distribution (Figure 5B).

The pairwise RS analysis is likewise consistent with a similar covariance pattern across most of the samples (Figure 6), as comparisons between age-specific **P**-matrices and the adult **P**-matrix yielded high similarity values ($RS > 0.81$), the exceptions being the age classes d20 and d40 for *Monodelphis* (B) ($RS = 0.64, RS = 0.73$, respectively). The RS comparison between age-specific **P**-matrices and target **G**-matrices presented a very similar result to the comparison with adult **P**-matrices, except that similarity values tended to be slightly lower ($RS > 0.69$). Exceptions were *Sapajus*, which wielded consistently lower similarity values than the comparison with the adult's **P**-matrix ($0.68 < RS < 0.79$), and *Monodelphis* (B), which showed lower values in general, and particularly for the two younger age classes ($RS < 0.44$). In the case of

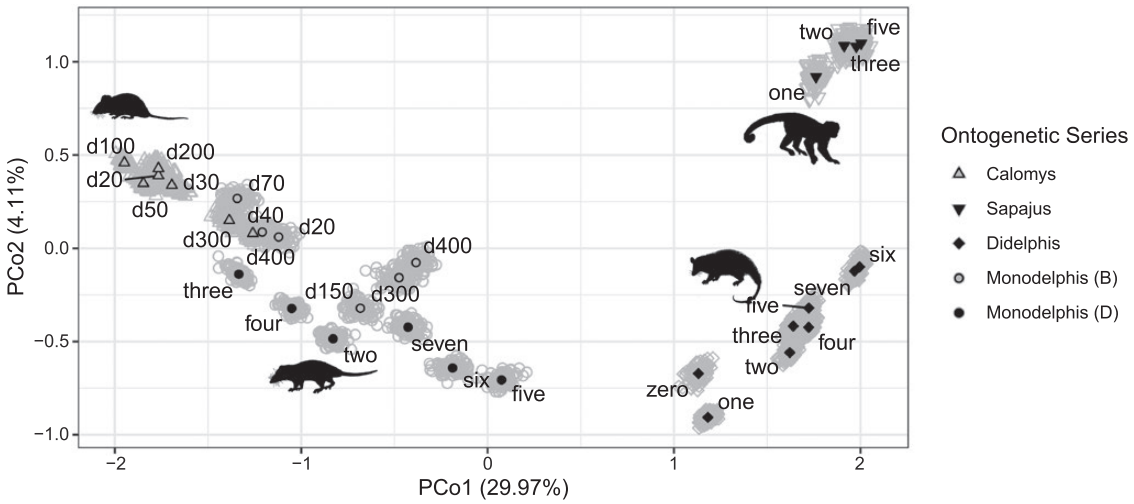

Figure 4. Distribution of age-specific **P**-matrices on the first two leading principal coordinates based on the Riemannian distance. Black symbols represent the median of each posterior distribution of age-specific **P**-matrices within each ontogenetic series. Gray symbols represent 100 matrices from the posterior distribution of age-specific **P**-matrices within each ontogenetic series. Figures not to scale.

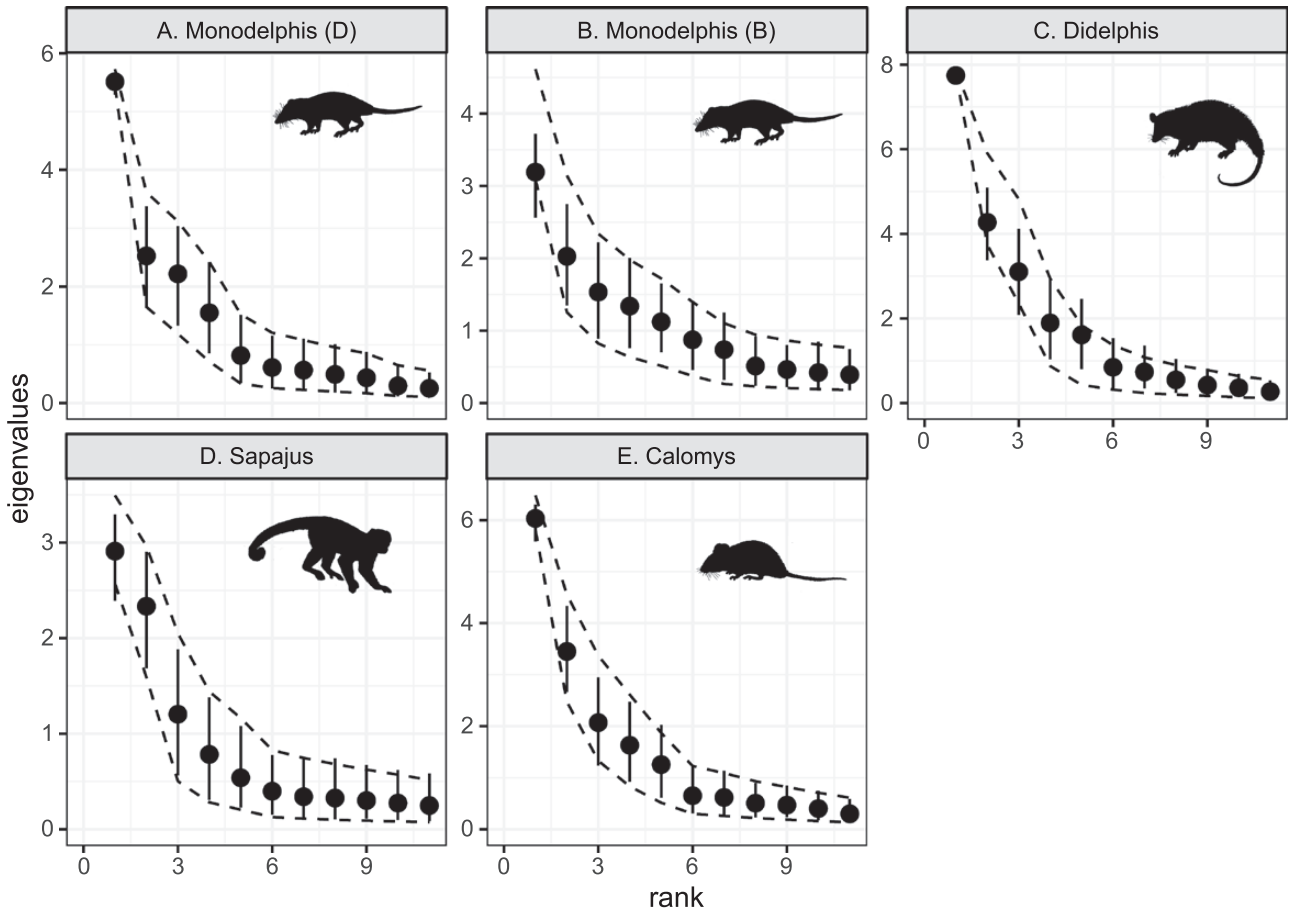

Figure 5. Distribution of the empirical (bars) and null (dashed lines) distributions of the eigenvalues of the Krzanowski Subspace Comparison for each ontogenetic series. Overlap between empirical and null eigenvalue distributions indicates that observed covariance matrices are as similar as matrices in which age class was randomized across individuals. While not identical, this is evidence that observed matrices are compatible with a single underlying covariance structure across age classes. Figures not to scale.

Sapajus, these lower similarities are still remarkably high considering that they are being compared to a **G**-matrix estimated for a species of a different family (Callitrichidae).

Low ratios between sample size and number of traits introduce errors in covariance matrix estimation (Marroig et al., 2012). In terms of matrix comparisons, poor sampling usually causes a decrease in the similarity between two matrices [Supplementary Figures A7–A9; Hubbe et al. (2016); Machado et al. (2018)]. Thus, despite sampling error, the high similarities we measure point to a biological signal. If

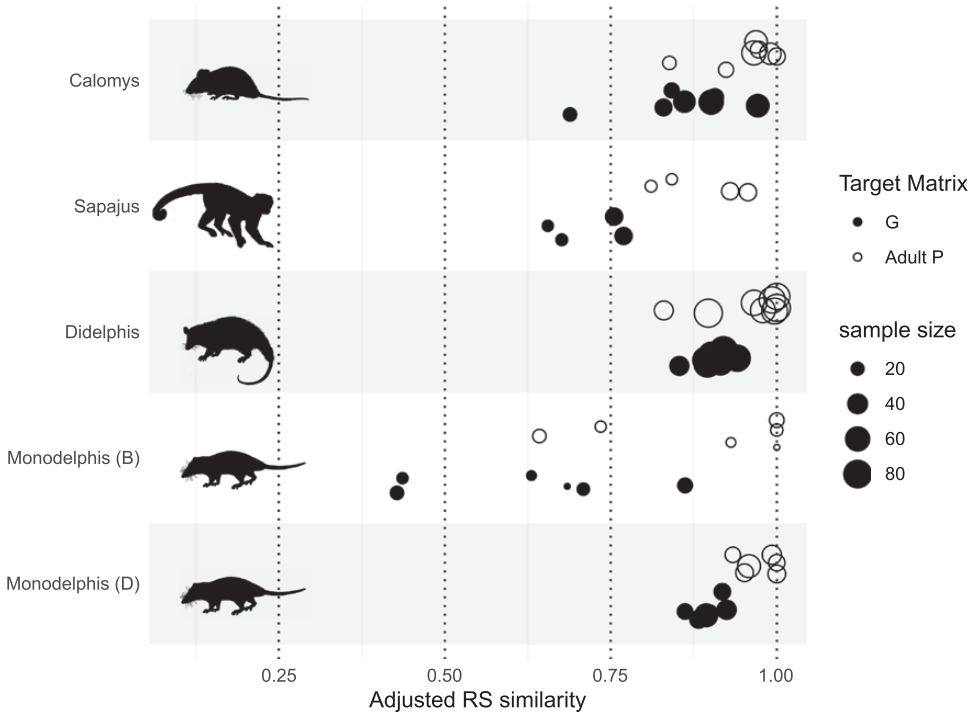

Figure 6. Distribution of adjusted random skewers similarity for each ontogenetic series between age-specific covariance **P**-matrices and a target matrix [adult **P**-matrix (upper row; transparent dots) and **G**-matrix (lower row; black dots); see details about those matrices in "Methods"]. Figures not to scale.

matrices were not biologically similar, sampling error would not increase the similarity of otherwise dissimilar matrices. Furthermore, the matrix repeatability method used to adjust the RS similarities tends to overestimate repeatabilities for poorly estimated **P**-matrices, leading to conservative corrections of matrices comparisons when poorly estimated **P**-matrix are involved. Therefore, we expect the RS values involving poorly estimated matrices to be underestimated.

In order to rule out the possibility that our results are driven by sampling error due to a small ratio of samples per trait, we also repeated our analysis using fewer traits. By using only 5 or 15 well-estimated traits (Supplementary Table A2), we aim to improve the relative sample size and reduce matrix estimation error. Our findings of overall similarity of covariance patterns during post-weaning stages for 35 traits are consistent with the analyses that used fewer traits. The Krzanowski Subspace Comparisons are essentially indistinguishable from the analysis of the full trait set (Supplementary Figures A10 and A11). For the RS analysis, matrices were shown to be actually more similar to both adult **P**s and target **G**s than in the full trait set (Supplementary Figures A8 and A9). Given that these reduced trait sets exclude the traits with lower repeatabilities, this suggests that a large fraction of the lower values in the original RS comparisons might be due to sampling error. Alternatively, because low repeatabilities are present on smaller traits, this could also be the case that differences between matrices are restricted to covariances involving smaller traits and that overall patterns of variation implied by large traits (length of rostrum, size of parietal, etc.) are conserved, while localized variation is not always similar.

Another point of concern is whether the clearly lower RS values for the birth age classes 20 and 40 for *Monodelphis* (B) are the results of sampling error. These matrices are among the worst estimates we have, which may suggest that sampling error dominated the matrix estimate. However, we posit that the lower similarity values for these age classes reflect some biological signals for two reasons. First, all **P**-matrices of *Monodelphis* (B) can be considered poorly estimated (Figure 2), and it is suggestive that the only matrix similarities lower than < 0.75 were the ones involving the two youngest age classes (Figure 6). Second, we did a Monte-Carlo rarefaction analysis of the *Monodelphis* (B) median **P**-matrix of the posterior distribution for adults (Figure A7). Solid lines represent 95% confidence intervals for the RS statistics based on the resampling of the *Monodelphis* (B) posterior median adult matrix using different sample sizes. Dashed lines represent the comparisons of the two posterior median younger age classes (20 and 40) **P**-matrices against the posterior median adult **P**-matrix. If the sample size was the main cause for differences in **P**-matrices patterns, we would expect that the Random Skewers value for **P**-matrices between birth age classes 20 or 40 and adult would fall within the confidence interval. Since this is not the case, at least part of the observed results is not due to sampling artifacts.

Discussion

In this contribution, we have investigated how the covariance pattern of mammalian cranial traits changes during the postnatal ontogeny in five ontogenetic series of four mammalian species, which show substantial life history and pre- and post-natal development differences (Smith, 1997). Our work shows that covariance patterns from weaning onward are fairly stable within ontogenetic series (Figures 5 and 6), and these patterns are largely driven by the same processes governing the (co)inheritance of traits (Figure 6), which suggest that the Cheverud Conjecture holds for covariance patterns during all post-weaning development, not only for adults as previously reported (Akesson et al., 2007; Cheverud, 1988, 1996b; House & Simmons, 2005; Porto et al., 2009; Reusch

& Blanckenhorn, 1998; Roff, 1995). Furthermore, the extension of the Cheverud conjecture throughout the ontogeny suggests that similar selective pressures operating on different life history stages will probably result in a similar evolutionary response.

One potential exception to this general pattern is *Monodelphis* (B). While the KC failed to find any significant difference between age classes, this ontogenetic series was the only case where a substantial part of the posterior distribution of eigenvalues of the common subspace matrix (**H**-matrix) fell outside the null distribution (Figure 5B, first eigenvalue). Furthermore, the leading axis of the PCoA is mainly associated with ontogenetic differences within *Monodelphis*, and Didelphimorphia to a lesser degree (Figure 4) and the RS showed differences during the lactation phase, at birth age classes d20 and d40 (Figure 6). At these early postnatal stages, covariance patterns were shown to be different to some extent from the patterns of additive genetic covariance as well (Figure 6). This suggests that at least for this group, the cranial trait covariance is subject to changes during the early stages of postnatal development, which stabilizes only around weaning. Nevertheless, probably due to low sample sizes, specific investigation into how trait covariances are changing between age classes are unfortunately inconclusive (Supplementary Figures A12 and A13).

In contrast, *Didelphis* during lactation (dental age class zero) presented similar covariance patterns with older dental age classes, but this result could be the consequence of sampling specimens based on dental age classes. Specifically, by pooling individuals with different absolute ages within the same class, one might be artificially inflating the effect of size, forcing eigenvectors to align themselves with those of the latter stages. Consequently, in such cases, RS will detect high similarities between matrices (Porto et al., 2013; Rohlf, 2017). This issue is particularly relevant for age classes in which specimens are experiencing higher growth rates, since relatively small variation in absolute ages within the dental age class will result in a relatively large variance in size, as is the case for dental age class zero for *Didelphis* (Supplementary Figure A14). In fact, the leading eigenvector of the age class zero for *Didelphis* shows almost all loadings with the same signal, as expected for size (Jolicoeur, 1963), while the same is not true for age classes d20 and d40 of *Monodelphis* (B) (Supplementary Figure A15). For placental mammals (*Sapajus* and *Calomys*), we do not have samples before weaning (Figure 2), so it is unclear if the same pattern observed on *Monodelphis* could be extended to all therian mammals. More studies focusing on earlier ontogenetic stages, and on larger samples based on birth age classes will be required to better understand this phenomenon.

At this point, we cannot accurately measure changes in covariance patterns prior to weaning, and we can only speculate on the reasons for the maintenance of covariance patterns post-weaning. The mammalian postnatal ontogeny occurs over major life history phases (Abdala et al., 2001; McManus, 1974; Nievelt & Smith, 2005) that may influence development (Atchley, 1984; Hallgrímsson et al., 2009; Sibly et al., 2014; Zelditch, 1988), such as lactation, beginning of solid food ingestion, and weaning. The postnatal stage is also characterized by several changes in the cranium (Abdala et al., 2001; Flores et al., 2006; Zelditch et al., 1992), such as the faster growth of the viscerocranium in relation to the neurocranium, and the development of muscles of the masticatory apparatus to deal with solid food, which influences the growth of underlying bones (Kiliaridis, 1995). Nevertheless, most postnatal development is shaped by growth and muscle-bone interactions, which are relatively late developmental inputs (Hallgrímsson et al., 2007, 2009). Given that the covariance pattern observed in adult populations are the end result of several hierarchical developmental processes (Hallgrímsson et al., 2007, 2009), it is possible that events that occur later in development might have smaller effects on determining covariance patterns due to constraints imposed by early processes (Atchley, 1984) and thus may have limited influence over covariance patterns. Alternatively, these later stages can be shaping the covariance pattern, overwriting early developmental inputs (Hallgrímsson et al., 2009).

Irrespective of the reasons for the maintenance of post-weaning covariance patterns, our findings have important implications for evolutionary, developmental, genetic, and ecological studies. We showed that during lactation covariance patterns may vary considerably, at least in marsupials, but that from weaning onward, covariance patterns become relatively stable. Thus, for specimens spanning from weaning to adulthood, selection operating on different cranial postnatal ontogenetic stages might have similar consequences on the responses produced in terms of the pattern of changes in trait averages. However, since we employed global similarity statistics (Marroig et al., 2011), we cannot exclude the possibility of localized deviations from this global pattern. Since this was not the scope of our study, further investigation is necessary to explore this topic.

Given that during lactation individuals should be subjected to very different selective regimes than after weaning, our results are reassuring in that working with a single post-weaning ontogenetic stage will not lead to misleading conclusions when studying mammalian cranial traits. We suggest that the broad taxonomic and profoundly different pre- and postnatal developmental strategies encompassed by our sample imply that our results can be extended at least to most therian mammals. It is well established that cranial adult covariance matrices tend to be very similar among taxa within higher taxonomic levels (Hubbe et al., 2016; Machado et al., 2018; Marroig & Cheverud, 2001; Rossoni et al., 2019; Shirai & Marroig, 2010), so there is little reason to believe that evolutionary lineages with more similar developmental patterns, such as within placentals or marsupials, will have a higher influence of developmental changes over covariance patterns on this structure. However, one should view this generalization with caution for taxa that could be considered morphological oddities (e.g., giant anteaters, cetaceans, and elephants) or that present a differentiated post-weaning development in comparison to most placentals or marsupials. Another caveat is that we are essentially discussing morphological traits during ontogeny in mammals and our conclusions should not be extended at face value to other types of traits such as behavior or even morphological traits in other groups (Styga et al., 2019).

Conclusion

Our findings suggest that for therian mammals, the study of the life history changes and evolutionary consequences under selection (or genetic drift) is much facilitated by shared and common covariance patterns among traits from weaning onward. Thus, even though selection might be operating in different directions during this period, due to differences in

life history phases and fitness components, the net response to such pressures will probably not be biased by differences in the covariance pattern during this period of postnatal ontogeny.

While our findings support using a single post-weaning ontogenetic stage in the investigation of selective pressures and evolutionary responses, they also highlight the need for a more comprehensive understanding of how covariances change between birth and weaning. In addition, it is important to better understand species life histories to evaluate when and how the selection is operating, since selective explanations inferred from adult morphologies might be a consequence of selection operating on other life stages. This is particularly relevant if species show a relatively drastic change in some ecological aspect during ontogeny [e.g., Drago et al. (2009); Tanner et al. (2010)]. Lastly, a full account of how changes in selective pressures during ontogeny can impact the response to selection would require considering the covariances for the same trait across ontogenetic stages as well. This requires longitudinal morphological data on the animals, which is a challenging but interesting venue for future research.

Supplementary material

Supplementary material is available online at *Evolution* (https://academic.oup.com/evolut/qpac052)

Data availability

Data necessary to replicate these results are publicly available at https://doi.org/10.5061/dryad.wstqjq2qs.

Author contributions

A.H.: conceptualization, data curation, formal analysis, investigation, methodology, visualization, writing—original draft and writing—review and editing, funding acquisition; F.A.M.: conceptualization, data curation, formal analysis, investigation, methodology, visualization, writing—original draft and writing—review and editing; D.M.: conceptualization, formal analysis, investigation, methodology, visualization, writing—original draft and writing—review and editing; G.G.: conceptualization, data acquisition, data curation, formal analysis, investigation, methodology, visualization, writing—review and editing, funding acquisition; H.S.: conceptualization, data acquisition, data curation, writing—review and editing, funding acquisition; A.P.: conceptualization, data acquisition, data curation, formal analysis, writing—review and editing, funding acquisition; J.C.: conceptualization, writing—review and editing, funding acquisition; G.M.: conceptualization, data acquisition, writing—review and editing, funding acquisition.

Conflict of interest: Editorial decisions were made independently of G.M., who is an Associate Editor of Evolution.

Acknowledgments

The authors are thankful to people and institutions that provided generous help and access to collections: A. Fleming, R. MacPhee, R. Voss, and E. Westwig (American Museum of Natural History); B. Patterson, L. Heaney, and B. Stanley (Field Museum of Natural History); S. Costa and J. de Queiros (Museu Paraense Emilio Goeldi); F. Barbosa, S. Franco, J. A. de Oliveira, and L. Salles (Museu Nacional); C. Conroy, E. Lacey, and J. Patton (Museum of Vertebrate Zoology); M. Brett-Surman, R. Chapman, L. Gordon, and D. Lunde (National Museum of Natural History); J. Gualda and M. de Vivo (Museu de Zoologia da Universidade de São Paulo); and J. VandeBerg (Texas Biomedical Research Institute). We are deeply indebted to four anonymous reviewers, P. David Polly and editors for their insightful comments on a previous draft of this manuscript. We are also thankful to Mark Hubbe, who kindly assisted with Figure 3. This research was supported by grants and fellowships from Fundação de Amparo à Pesquisa do Estado de São Paulo (FAPESP), Coordenadoria de Aperfeiçoamento de Pessoal de Nível Superior (CAPES), Conselho Nacional de Desenvolvimento Científico e Tecnológico (CNPq), Museum of Vertebrate Zoology (UC-Berkeley), American Museum of Natural History, Field Museum of Natural History, and NSF (DEB 1942717).

References

Abdala, F., Flores, D. A., & Giannini, N. P. (2001). Postweaning ontogeny of the skull of Didenphis albiventris. *Journal of Mammalogy*, 82(1), 190–200. https://doi.org/10.1093/jmammal/82.1.190

Aguirre, J. D., Hine, E., McGuigan, K., & Blows, M. W. (2014). Comparing G: Multivariate analysis of genetic variation in multiple populations. *Heredity*, 112(1), 21–29.

Akesson, M., Bensch, S., & Hasselquist, D. (2007). Genetic and phenotypic associations in morphological traits: A long term study of great reed warblers *Acrocephalus arundinaceus*. *Journal of Avian Biology*, 38(1), 58–72.

Anderson, M. J. (2001). A new method for non-parametric multivariate analysis of variance. *Austral Ecology*, 26(11), 32–46. https://doi.org/10.1111/j.1442-9993.2001.01070.pp.x

Assis, A. P. A., Galetti, M., Maia, K. P., & Guimarães, P. R. (2022). Reduced evolutionary potential of a frugivorous bird species in fragmented forests. *Frontiers in Ecology and Evolution*, 10, 804138.

Atchley, W. R. (1984). Ontogeny, timing of development, and genetic variance-covariances structure. *The American Naturalist*, 123(44), 519–540. https://doi.org/10.1086/284220

Bookstein, F. L., & Mitteroecker, P. (2014). Comparing covariance matrices by relative eigenanalysis, with applications to organismal biology. *Evolutionary Biology*, 41(2), 336–350.

Cheverud, J. M. (1982). Phenotypic, genetic, and environmental morphological integration in the cranium. *Evolution*, 36(33), 499–516. https://doi.org/10.2307/2408096

Cheverud, J. M. (1988). A comparison of genetic and phenotypic correlations. *Evolution*, 42(55), 958–968. https://doi.org/10.2307/2408911

Cheverud, J. M. (1995). Morphological integration in the Saddle-back Tamarin (*Saguinus fuscicollis*) cranium. *The American Naturalist*, 145(11): 63–89. https://doi.org/10.1086/285728

Cheverud, J. M. (1996a). Developmental integration and the evolution of pleiotropy. *American Zoologist*, 36(11), 44–50. https://doi.org/10.1093/icb/36.1.44

Cheverud, J. M. (1996b). Quantitative genetic analysis of cranial morphology in the cotton-top (*Saguinus oedipus*) and saddle-back (*S. fuscicollis*) tamarins. *Journal of Evolutionary Biology*, 9(11), 5–42. https://doi.org/10.1046/j.1420-9101.1996.9010005.x

Cheverud, J. M., & Marroig, G. (2007). Comparing covariance matrices: Random skewers method compared to the common principal components model. *Genetics and Molecular Biology*, 30(22), 461–469. https://doi.org/10.1590/s1415-47572007000300027

Coleman, J. S., McConnaughay, K. D., & Ackerly, D. D. (1994). Interpreting phenotypic variation in plants. *Trends in Ecology & Evolution*, 9(5), 187–191.

Collyer, M. L., & Adams, D. C. (2018). RRPP: An r package for fitting linear models to high-dimensional data using residual randomization. *Methods in Ecology and Evolution*, 9(7), 1772–1779.

Drago, M., Cardona, L., Crespo, E. A., & Aguilar, A. (2009). Ontogenic dietary changes in South American sea lions. *Journal of Zoology*, 279(33): 251–261. https://doi.org/10.1111/j.1469-7998.2009.00613.x

Eisenberg, J. F. (1989). *Mammals of the Neotropics, Volume 1: The Northern Neotropics: Panama, Colombia, Venezuela, Guyana, Suriname, French Guiana*. The University of Chicago Press.

Eisenberg, J. F., & Redford, K. H. (1999). *Mammals of the Neotropics, Volume 3: The Central Neotropics: Ecuador, Peru, Bolivia, Brazil*. The University of Chicago Press.

Falconer, D. S., & MacKay, T. F. C. (1996). *Introduction to quantitative genetics*. Longman.

Flores, D. A., Giannini, N., & Abdala, F. (2006). Comparative postnatal ontogeny of the skull in the australidelphian metatherian *Dasyurus albopunctatus* (Marsupialia: Dasyuromorpha: Dasyuridae). *Journal of Morphology*, 267(44), 426–440. https://doi.org/10.1002/jmor.10420

Forester, B. R., Beever, E. A., Darst, C., Szymanski, J., & Funk, W. C. (2022). Linking evolutionary potential to extinction risk: Applications and future directions. *Frontiers in Ecology and the Environment*, 20(9), 507–515. https://onlinelibrary.wiley.com/doi/pdf/10.1002/fee.2552.

Fragazy, D. M., Visalberghi, E., & Fedigan, L. M. (2004). *The Complete Capuchin: The Biology of the Genus Cebus*. Cambridge University Press.

Garcia, G., Hingst-Zaher, E., Cerqueira, R., & Marroig, G. (2014). Quantitative Genetics and modularity in cranial and mandibular morphology of *Calomys expulsus*. *Evolutionary Biology*, 41(44), 619–636. https://doi.org/10.1007/s11692-014-9293-4

Gervais, L., Perrier, C., Bernard, M., Merlet, J., Pemberton, J. M., Pujol, B., & Qu, E. (2019). RAD-sequencing for estimating genomic relatedness matrix-based heritability in the wild: A case study in roe deer. *Molecular Ecology Resources*, 19(5), 1205–1217. Wiley Online Library.

Goswami, A. (2006). Morphological integration in the carnivoran skull. *Evolution*, 60(11), 169–183. https://doi.org/10.1554/05-110.1

Goswami, A., Polly, P. D., Mock, O. B., & SÁNchez-Villagra, M. R. (2012). Shape, variance and integration during craniogenesis: Contrasting marsupial and placental mammals. *Journal of Evolutionary Biology*, 25(55), 862–872. https://doi.org/10.1111/j.1420-9101.2012.02477.x

Haber, A. (2015). The evolution of morphological integration in the ruminant skull. *Evolutionary Biology*. 42, 99–114.

Hallgrímsson, B., Jamniczky, H., Young, N. M., Rolian, C., Parsons, T. E., Boughner, J. C., & Marcucio, R. S. (2009). Deciphering the palimpsest: Studying the relationship between morphological integration and phenotypic covariation. *Evolutionary Biology*, 36(44), 355–376. https://doi.org/10.1007/s11692-009-9076-5

Hallgrímsson, B., Lieberman, D. E., Young, N. M., Parsons, T., & Wat, S. (2007). Evolution of covariance in the mammalian skull. In G. Bock, & J. Goode (Eds.), *Tinkering: The microevolution of development* (pp. 164–190). John Wiley & Sons, Ltd.

Hingst-Zaher, E., Marcus, L. F., & Cerqueira, R. (2000). Application of geometric morphometrtcs to the study of postnatal size and shape changes in the skull of *Calomys expdsus*. *Hystrix*, 11(1), 99–113.

House, C. M., & Simmons, L. W. (2005). The evolution of male genitalia: Patterns of genetic variation and covariation in the genital sclerites of the dung beetle *Onthophagus taurus*. *Journal of Evolutionary Biology*, 18(5), 1281–1292. https://doi.org/10.1111/j.1420-9101.2005.00926.x

Hubbe, A., Melo, D., & Marroig, G. (2016). A case study of extant and extinct *Xenarthra cranium* covariance structure: Implications and applications to paleontology. *Paleobiology*, 42(33), 465–488. https://doi.org/10.1017/pab.2015.49

Jolicoeur, P. (1963). 193. Note: The multivariate generalization of the allometry equation. *Biometrics*, 19(33), 497–499. https://doi.org/10.2307/2527939

Jones, K. E., Bielby, J., Cardillo, M., Fritz, S. A., O'Dell, J., Orme, C. D. L., Safi, K., Sechrest, W., Boakes, E. H., Carbone, C., Connolly, C., Cutts, M. J., Foster, J. K., Grenyer, R., Habib, M., Plaster, C. A., Price, S. A., Rigby, E. A., Rist, J., … Purvis, A. (2009). PanTHERIA: A species-level database of life history, ecology, and geography of extant and recently extinct mammals. *Ecology*, 90(99), 2648–2648. https://doi.org/10.1890/08-1494.1

Kiliaridis, S. (1995). Masticatory muscle influence on craniofacial growth. *Acta Odontologica Scandinavica*, 53(33), 196–202. https://doi.org/10.3109/00016359509005972

Konigsberg, L. W., & Cheverud, J. M. (1992). Uncertain paternity in primate quantitative genetic studies. *American Journal of Primatology*, 27(22), 133–143. https://doi.org/10.1002/ajp.1350270208

Krzanowski, W. J. (1979). Between-groups comparison of principal components. *Journal of the American Statistical Association*, 74(367), 703–707.

Lande, R. (1979). Quantitative genetic analysis of multivariate evolution, applied to brain: Body size allometry. *Evolution*, 33(11), 402–416. https://doi.org/10.2307/2407630

Lande, R., & Arnold, S. J. (1983). The measurement of selection on correlated characters. *Evolution*, 37(66), 1210–1226. https://doi.org/10.2307/2408842

Le Maître, A., & Mitteroecker, P. (2019). Multivariate comparison of variance in r. *Methods in Ecology and Evolution*, 10(99), 1380–1392. https://doi.org/10.1111/2041-210x.13253

Lessells, C. M., & Boag, P. T. (1987). Unrepeatable repeatabilities: A common mistake. *Auk*, 104(1), 116–121.

Machado, F. A., Zahn, T. M. G., & Marroig, G. (2018). Evolution of morphological integration in the skull of Carnivora (Mammalia): Changes in Canidae lead to increased evolutionary potential of facial traits. *Evolution*, 72(77), 1399–1419. https://doi.org/10.1111/evo.13495

Marroig, G. (2007). When size makes a difference: Allometry, life-history and morphological evolution of capuchins (Cebus) and squirrels (Saimiri) monkeys (Cebinae, Platyrrhini). *BMC Evolutionary Biology*, 7, 20.

Marroig, G., & Cheverud, J. M. (2001). A comparison of phenotypic variation and covariation patterns and the role of phylogeny. Ecology, and ontogeny during cranial evolution of new world monkeys. *Evolution*, 55(1212), 2576–2600. https://doi.org/10.1554/0014-3820(2001)055[2576:acopva]2.0.co;2

Marroig, G., & Cheverud, J. (2010). Size as a line of least resistance II: Direct selection on size or correlated response due to constraints? *Evolution*, 64(5), 1470–1488.

Marroig, G., Melo, D. A. R., & Garcia, G. (2012). Modularity, noise, and natural selection. *Evolution*, 66(55), 1506–1524. https://doi.org/10.1111/j.1558-5646.2011.01555.x

Marroig, G., Melo, D., Porto, A., Sebastiao, H., & Garcia, G. (2011). Selection response decomposition (SRD): A new tool for dissecting differences and similarities between matrices. *Evolutionary Biology*, 38(22), 225–241. https://doi.org/10.1007/s11692-010-9107-2

McArdle, B. H., & Anderson, M. J. (2001). Fitting multivariate models to community data: A comment on distance-based redundancy analysis. *Ecology*, 82(1), 290–297. https://doi.org/10.1890/0012-9658(2001)082[0290:fmmtcd]2.0.co;2

McGuigan, M. C. (2006). Studying phenotypic evolution using multivariate quantitative genetics. *Molecular Ecology*, 15(4), 883–896.

McManus, J. (1974). *Didelphis virginiana*. *Mammalian Species*, 40, 1–6.

Melo, D., Garcia, G., Hubbe, A., Assis, A., & Marroig, G. (2015). EvolQG—An R package for evolutionary quantitative genetics [version 1; referees: awaiting peer review]. *F1000Research*, 4, 925.

Mitteroecker, P. (2009). The developmental basis of variational modularity: Insights from quantitative genetics, morphometrics, and developmental biology. *Evolutionary Biology*, 36(4), 377–385. https://doi.org/10.1007/s11692-009-9075-6

Mitteroecker, P., & Bookstein, F. (2009). The ontogenetic trajectory of the phenotypic covariance matrix, with examples from craniofacial

shape in rats and humans. *Evolution*, 63(33), 727–737. https://doi.org/10.1111/j.1558-5646.2008.00587.x
Mitteroecker, P., Gunz, P., Neubauer, S., & Mueller, G. (2012). How to explore morphological integration in human evolution and development? *Evolutionary Biology*, 39(4), 536–553.
Murphy, K. P. (2012). *Machine learning: a probabilistic perspective*. MIT press.
Nievelt, A. F. H. V., & Smith, K. K. (2005). To replace or not to replace: The significance of reduced functional tooth replacement in marsupial and placental mammals. *Paleobiology*, 31(2), 324–346. Paleontological Society.
Nonaka, K., & Nakata, M. (1984). Genetic variation and craniofacial growth in inbred rats. *Journal of Craniofacial Genetics and Developmental Biology*, 4(4), 271–302.
Oliveira, F. B., Porto, A., & Marroig, G. (2009). Covariance structure in the skull of Catarrhini: A case of pattern stasis and magnitude evolution. *Journal of Human Evolution*, 56(4), 417–430.
Olson, E. C., & Miller, R. L. (1958). *Morphological integration*. University of Chicago Press.
Porto, A., Oliveira, F. B. D., Shirai, L. T., Conto, V. D., & Marroig, G. (2009). The evolution of modularity in the mammalian skull I: Morphological integration patterns and magnitudes. *Evolutionary Biology*, 36, 118–135.
Porto, A., Sebastião, H., Pavan, S. E., VandeBerg, J. L., Marroig, G., & Cheverud, J. M. (2015). Rate of evolutionary change in cranial morphology of the marsupial genus *Monodelphis* is constrained by the availability of additive genetic variation. *Journal of Evolutionary Biology*, 28(44), 973–985. https://doi.org/10.1111/jeb.12628
Porto, A., Shirai, L. T., de Oliveira, F. B., & Marroig, G. (2013). Size variation, growth strategies, and the evolution of modularity in the mammalian skull. *Evolution*, 67(1111), 3305–3322. https://doi.org/10.1111/evo.12177
Porto, A. S. (2009). *Evolução da modularidade no crânio de mamíferos*. Master Dissertation, Universidade de São Paulo, São Paulo.
R Core Team. (2019). *R: A Language and Environment for Statistical Computing*. R Foundation for Statistical Computing, Vienna, Austria.
Redford, K. H., & Eisenberg, J. F. (1992). *Mammals of the Neotropics, Volume 2: The Southern Cone: Chile, Argentina, Uruguay, Paraguay*. University of Chicago Press.
Reusch, T., & Blanckenhorn, W. U. (1998). Quantitative genetics of the dung fly *Sepsis cynipsea*: Cheverud's conjecture revisited. *Heredity*, 81(11), 111–119. https://doi.org/10.1046/j.1365-2540.1998.00368.x
Richtsmeier, J. T., Corner, B. D., Grausz, H. M., Cheverud, J. M., & Danahey, S. E. (1993). The role of postnatal growth pattern in the production of facial morphology. *Systematic Biology*, 42(33), 307–330. https://doi.org/10.2307/2992466
Roff, D. A. (1995). The estimation of genetic correlations from phenotypic correlations: A test of Cheverud's conjecture. *Heredity*, 74(5), 481–490. https://doi.org/10.1038/hdy.1995.68
Rohlf, F. J. (2017). The method of random skewers. *Evolutionary Biology*, 44(44), 542–550. https://doi.org/10.1007/s11692-017-9425-8
Rossoni, D. M., Costa, B. M. A., Giannini, N. P., & Marroig, G. (2019). A multiple peak adaptive landscape based on feeding strategies and roosting ecology shaped the evolution of cranial covariance structure and morphological differentiation in phyllostomid bats. *Evolution*, 73(55), 961–981. https://doi.org/10.1111/evo.13715
Runcie, D. E., & Mukherjee, S. (2013). Dissecting high-dimensional phenotypes with bayesian sparse factor analysis of genetic covariance matrices. *Genetics*, 194(33), 753–767. https://doi.org/10.1534/genetics.113.151217
Saccheri, I., & Hanski, I. (2006). Natural selection and population dynamics. *Trends in Ecology & Evolution*, 21(6), 341–347.
Sebastião, H., & Marroig, G. (2013). Size and shape in cranial evolution of 2 marsupial genera: Didelphis and Philander (Didelphimorphia, Didelphidae). *Journal of Mammalogy*, 94(66), 1424–1437. https://doi.org/10.1644/11-mamm-a-349.1
Shirai, L. T., & Marroig, G. (2010). Skull modularity in neotropical marsupials and monkeys: Size variation and evolutionary constraint and flexibility. *Journal of Experimental Zoology. Part B. Molecular and Developmental Evolution*, 314B(8), 663–683.
Sibly, R. M., Grady, J. M., Venditti, C., & Brown, J. H. (2014). How body mass and lifestyle affect juvenile biomass production in placental mammals. *Proceedings of the Royal Society B: Biological Sciences*, 281(1777): 20132818. https://doi.org/10.1098/rspb.2013.2818
Smith, K. K. (1997). Comparative patterns of craniofacial development in Eutherian and Metatherian mammals. *Evolution*, 51(5), 1663–1678. https://doi.org/10.2307/2411218
Steppan, S. J., Phillips, P. C., & Houle, D. (2002). Comparative quantitative genetics: Evolution of the G matrix. *Trends in Ecology & Evolution*, 17(7), 320–327.
Styga, J. M., Houslay, T. M., Wilson, A. J., & Earley, R. L. (2019). Development of G: A test in an amphibious fish. *Heredity*, 122(5), 709696–709710. https://doi.org/10.1038/s41437-019-0193-3
Sydney, N. V., Machado, F. A., & Hingst-Zaher, E. (2012). Timing of ontogenetic changes of two cranial regions in *Sotalia guianensis* (Delphinidae). *Mammalian Biology*, 77(6), 397–403. https://doi.org/10.1016/j.mambio.2012.04.007. Publisher: Springer.
Tanner, J. B., Zelditch, M. L., Lundrigan, B. L., & Holekamp, K. E. (2010). Ontogenetic change in skull morphology and mechanical advantage in the spotted hyena (*Crocuta crocuta*). *Journal of Morphology*, 271(3), 353–365.
Tribe, C. J. (1990). Dental age classes in *Marmosa incana* and other didelphoids. *Journal of Mammalogy*, 71(44), 566–569. https://doi.org/10.2307/1381795
Tyndale-biscoe, C. H., & Mackenzie, R. B. (1976). Reproduction in *Didelphis marsupialis* and *Didelphis albiventris* in Colombia. *Journal of Mammalogy*, 57(22), 249–265. https://doi.org/10.2307/1379686
van Nievelt, A. F. H., & Smith, K. K. (2005). Tooth eruption in *Monodelphis domestica* and its significance for phylogeny and natural history. *Journal of Mammalogy*, 86(2), 333–341. https://doi.org/10.1644/bwg-224.1
VandeBerg, J. L., & Robinson, E. S. (1997). The laboratory opossum (*Monodelphis domestica*) in laboratory research. *ILAR Journal*, 38(11), 4–12. https://doi.org/10.1093/ilar.38.1.4
Wasserman, B. A., Reid, K., Arredondo, O. M., Osterback, A. K., Kern, C. H., Kiernan, J. D., & Palkovacs, E. P. (2021). Predator life history and prey ontogeny limit natural selection on the major armour gene, Eda, in threespine stickleback. *Ecology of Freshwater Fish*. 31(2), 291–299.
Zelditch, M. L. (1988). Ontogenetic variation in patterns of phenotypic integration in the laboratory rat. *Evolution*, 42(11), 28–41. https://doi.org/10.2307/2409113
Zelditch, M. L., Bookstein, F. L., & Lundrigan, B. L. (1992). Ontogeny of integrated skull growth in the cotton rat *Sigmodon fulviventer*. *Evolution*, 46(44), 1164–1180. https://doi.org/10.2307/2409763
Zelditch, M. L., & Carmichael, A. C. (1989). Ontogenetic variation in patterns of developmental and functional integration in skulls of *Sigmodon fulviventer*. *Evolution*, 43(44), 814–824. https://doi.org/10.2307/2409309
Zelditch, M. L., Mezey, J., Sheets, H. D., Lundrigan, B. L., & Garland, T. (2006). Developmental regulation of skull morphology II: Ontogenetic dynamics of covariance. *Evolution & Development*, 8(1), 46–60.